Observation of suppression of heavy-ion fusion by slow quasifission

L. T. Bezzina[1,*], *E. C.* Simpson[1], *D. J.* Hinde[1], and *M.* Dasgupta[1]

[1]Department of Nuclear Physics and Accelerator Applications, The Australian National University

Abstract.
The formation of superheavy elements (SHEs) by nuclear fusion can be conceptually divided into two steps: capture, and compound nucleus formation. Once captured, the two nuclei may reseparate before fusing to form a compact compound nucleus. This outcome is called quasifission.
Fusion-fission, in many cases, leads to reactions outcomes inseparable from quasifission. Evaporation residue (ER) measurements are therefore the most reliable, direct experimental signature of fusion. ER cross section measurements forming the same compound nucleus, ^{220}Th, using ^{16}O, ^{40}Ar, ^{48}Ca, ^{82}Se and ^{124}Sn-induced reactions [1–4] revealed [1] that fusion was severely suppressed for the more symmetric reactions relative to the ^{16}O-induced reaction.
Here two new reactions forming ^{220}Th using ^{28}Si, ^{34}S projectiles provide conclusive evidence that the ER cross section is exponentially suppressed as a function of Z_pZ_t. The fission characteristics show no mass-angle correlation, demonstrating that here ER cross sections are suppressed by slow quasifission.

1 Introduction

The formation of superheavy elements (SHEs) by heavy ion fusion is a fundamental challenge to our understanding of both experimental and theoretical nuclear reactions, and one that has been a well-explored topic of the FUSION series of conferences.

Figure 1 is an illustration of the reaction outcomes following a heavy-ion collision. While the ultimate aim of SHE synthesis is the formation of evaporation residues (ERs), it is well known that the other processes illustrated in this figure (deep inelastic collisions, quasifission and fusion-fission), compete with ER formation [5]. Previous studies have shown that the competition with these processes increases with the charge product in the entrance channel (Z_pZ_t), leading to suppression of the ER cross section. It is not always clear, however, how the relative probabilities of these competing processes evolves with Z_pZ_t.

While fusion-fission arises following the formation of an equilibrated compound nucleus (CN) - required for ER formation - quasifission results from reseparation of the dinuclear system before full equilibration has been reached. Quasifission on fast timescales can result in products which have a mass-angle correlation [6], but this correlation is typically lost once the dinuclear system has completed a rotation of 180° in the centre of mass frame, resulting in mass-angle characteristics which are indistinguishable from fusion-fission. This latter process has been termed slow quasifission [7].

This study takes advantage of the capabilities at the Australian Nation University to measure both ERs and detailed fission characteristics in order to investigate compound nucleus suppression in reactions resulting in slow quasifission.

This measurement scheme can be framed in the context of equation 1, which is a version of the commonly-used three factor expression of the ER cross section:

$$\sigma_{ER} = \pi\lambda^2 \sum_{l=0}^{\infty}(2l+1)T_l P_{CN}(E^*,l)W_{sur}(E^*,l). \quad (1)$$

Here, $\pi\lambda^2 \sum_{l=0}^{\infty}(2l+1)T_l$ embeds information about the capture process, which requires the system to have enough kinetic energy to overcome the electrostatic repulsion between the two nuclei, and stick together due to the attractive nuclear force. Once captured, the energy of the system is fully dissipated and shared between all the constituent nucleons. The T_l are the barrier-penetration probabilities. $P_{CN}(E^*,l)$ is the probability of reaching the compact compound nucleus after capture, and $W_{sur}(E^*,l)$ is the probability of ER survival against competition with fusion-fission.

By using cross bombardment reactions (where the same compound nucleus is formed using different beam-target combinations), and measuring only the ERs arising from neutron evaporation (xn ERs), we can obtain an unambiguous signature of CN formation (whereas nuclei arising from p and α evaporation can also be produced by incomplete charge capture of the projectile [8]). For the low l-values leading to xn ERs, it is expected that T_l is near unity at energies significantly above the capture barrier [9]. This means that W_{sur} should be the same for each reaction measured at the same (E^*, J), in accordance with Bohr's Independence Hypothesis [10].

*e-mail: lauren.bezzina@anu.edu.au

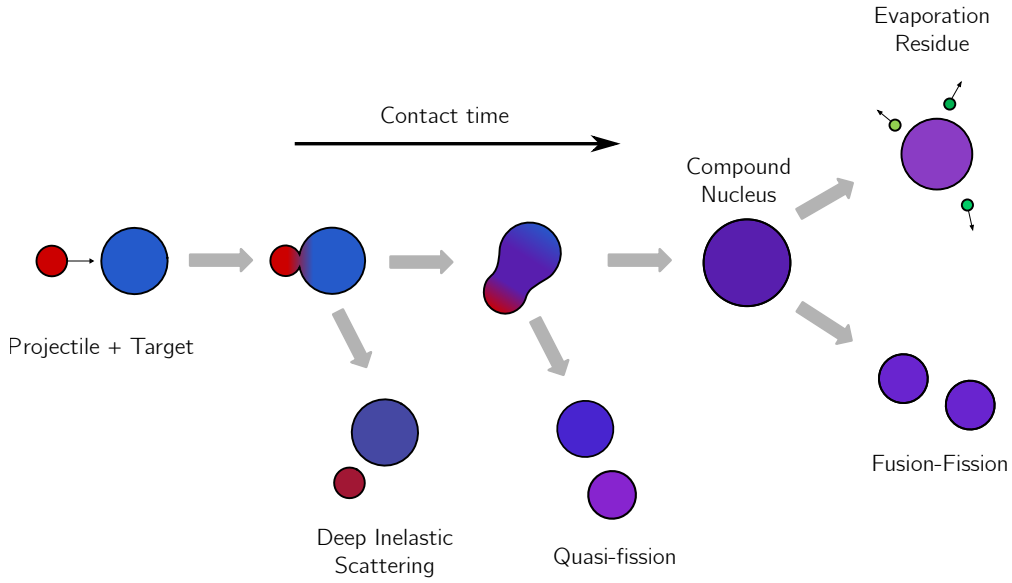

Figure 1. Illustrative diagram showing some of the reaction outcomes that may arise from heavy ion collisions.

Finally, by dividing the measured cross sections by $\pi\lambda^2$, we obtain the reduced cross section, $\widetilde{\sigma}_{xn}$. This quantity removes the kinematic effects of the entrance channel mass and energy, leaving a quantity which is directly proportional to P_{CN} - the probability of forming the compound nucleus. If a ratio of $\widetilde{\sigma}_{xn}$ can be taken to that of a system where it is known that P_{CN}=1, then one would be left with $\overline{P}_{CN}$: an average of P_{CN} over the low l that lead to ER formation.

The compound nucleus chosen for these cross bombardment reactions was ^{220}Th. This CN has the advantage of multiple formation pathways involving stable beam-target combinations, and ER cross sections which are relatively high (in comparison to many SHE studies). An additional benefit of this system was the existence of multiple prior measurements of both ER cross sections [1–4] and fission characteristics [11] - ensuring that comparisons could be made across 656< Z_pZ_t <2000.

2 ER cross sections by implantation-decay

The main experimental challenge involved in measuring ERs is separation from the large background of elastic scattering. Excellent separation of ERs from elastic scattering was achieved with the fusion-product separator SOLITAIRE [12], a device based on an 8 T superconducting solenoid, and depicted in Figure 2. The solenoid is filled with low-pressure helium gas, enabling separation of the relatively low-velocity ERs from the fast elastic events based on their average ionic charge state [13]. The device has a large angular acceptance of 86 msr, resulting in a transport efficiency of around 90% for the xn ERs measured in this study.

Following transport through the device, the ERs are implanted into a 50 mm × 50 mm silicon detector. As all the xn ERs produced by ^{220}Th decay predominantly via alpha decay, the well-defined alpha energies detected in the silicon can be used to identify the parent nucleus, while the number of decay-alphas can then be used to quantify the number of parent ERs and thus calculate σ_{xn}.

Implantation-decay spectra obtained for verification of this method are shown in Figure 3. Figure 3(a) shows the energy and arrival time of all events incident in the silicon detector for the benchmarking reaction of ^{30}Si+^{186}W at E_{beam} = 140 MeV whose cross section is known [9]. ERs, alpha decays, and elastically scattered events are labelled, with the ER events clearly separated in time from the elastically scattered contaminants. Figure 3(b) is the same data as in Figure 3(a), but with an anti-coincidence condition on the multiwire proportional counter (MWPC), removing most events originating from the target, leaving behind the decay-alphas and light prompt contaminants, which give only small signals in the MWPC.

After identifying and quantifying the decay-alpha spectrum, the cross section σ_{xn} and reduced cross section $\widetilde{\sigma}_{xn}$ can be calculated. $\widetilde{\sigma}_{xn}$ is plotted as a function of E^* in Figure 4 for the systems measured for this work (coloured symbols) as well as literature values for systems forming the same compound nucleus (symbols in grey scale) [1].

It is clear that the new systems measured for this work (^{28}Si+^{192}Os and ^{34}S+^{186}W) have a suppression intermediate to that of ^{16}O+^{204}Pb and the previously-measured systems. For a more quantitative measure of the suppression, we took the ratio of the reduced cross section for each data point in each system relative to a fit to the ^{16}O+^{204}Pb data shown by the full line. This gives the suppression of the xn

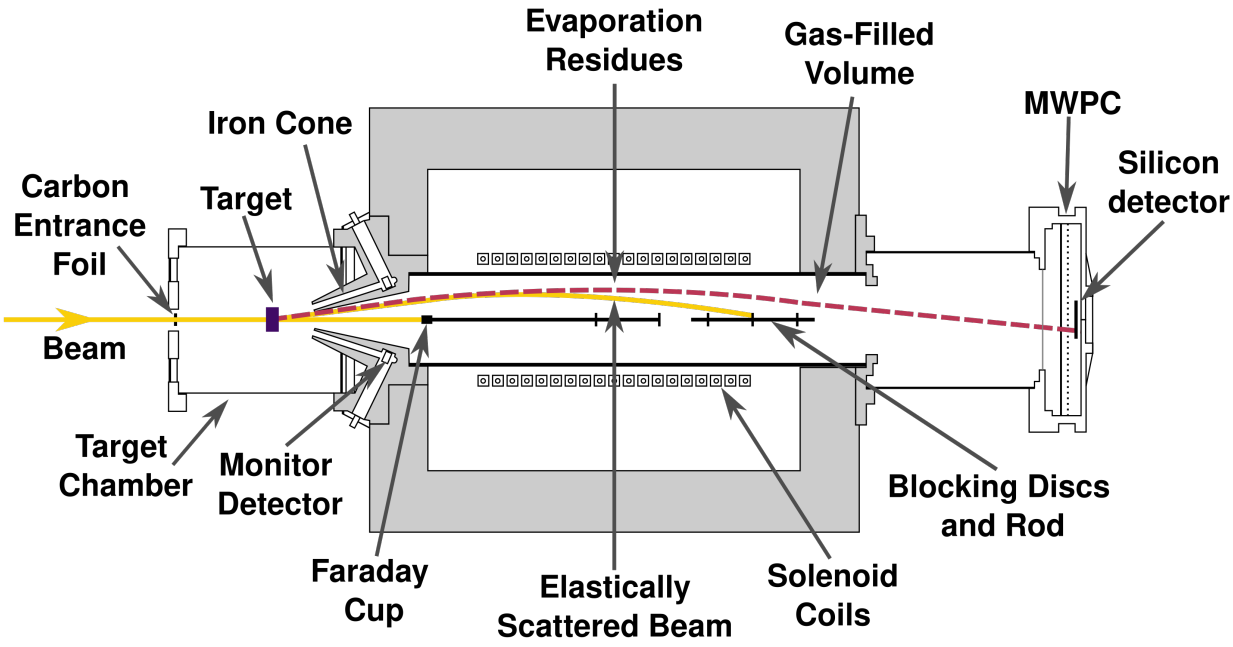

Figure 2. Schematic diagram of SOLITAIRE. This figure is adapted from [14], and shows key components of the device, as well as indicative radial trajectories of evaporation residues (red dashed line) and elastically scattered beam particles (orange line). The shaded grey area indicates the iron shielding of the solenoid, including the iron 'nose' cone at the solenoid entrance. Also indicated are two of the four monitor detectors used for normalisation to elastic scattering, the multiwire proportional counter (MWPC) used for direct detection of evaporation residues, and the silicon detector used for implantation-decay measurements.

cross section relative to ^{16}O+^{204}Pb, a quantity analogous to P_{CN}:

$$\text{Supppression} = \frac{\sigma_{xn}/\pi\lambda^2(\text{heavy projectile})}{\sigma_{xn}/\pi\lambda^2(\text{light projectile})} \quad (2)$$

$$= \frac{\widetilde{\sigma}_{xn}(^{N}\text{Z})}{\widetilde{\sigma}_{xn}(^{16}\text{O})}. \quad (3)$$

Note that this quantity is only *equal* to P_{CN} if we assert that there is no suppression in the reaction induced by the light projectile (in this instance, the ^{16}O+^{204}Pb reaction).

Figure 5 shows this ratio as a function of Z_pZ_t (coloured points) for all the systems shown in Figure 4, where the average over E^* has been evaluated. The overall trend is consistent with an exponential suppression of the CN formation probability with Z_pZ_t. This might originate from a reduction in capture probability (T_l in Equation 1) as well as a reduction in P_{CN}. To address this question, capture probabilities (averaged over all angular momenta) evaluated in Refs. [15] and [16] are shown by the hollow points. These show that the suppression of the ER cross sections is much larger than that of capture. The additional suppression must result from a process following capture, namely quasifission.

3 Fission characteristics

Turning then to fission characteristics, we present data measured with the ANU CUBE fission spectrometer [17]. This detector array, with unprecedented angular coverage, captures position and timing information of binary coincident events, enabling the reconstruction of the centre of mass angle and mass ratio of those events [17] (among other quantities) using the kinematic coincidence method [18]. A schematic view of the detector array is presented in Figure 6. Details of the MWPC design and analysis of CUBE data are covered in Refs. [17, 19].

CUBE fission spectrometer measurements were made for this work for the ^{16}O+^{204}Pb, ^{28}Si+^{192}Os, ^{34}S+^{186}W and ^{48}Ca+^{172}Yb systems. Following those measurements, the data were analysed and used to produce mass-angle distributions (MADs) these are presented in Figure 7, along with the reactions of ^{48}Ca+^{172}Yb and ^{50}Ti+^{170}Er [11] measured at similar excitation energy with the same detector system.

The defining characteristic of the MADs of the ^{28}Si+^{192}Os and ^{34}S+^{186}W systems is that there is *no* mass angle correlation present, despite the suppression in ER cross sections demonstrated in Figure 5. Without this mass-angle correlation, which is a distinct signature of fast quasifission [5, 6], this leaves slow quasifission as the only process which can lead to compound nucleus suppression. These results indicate that absence of a mass angle correlation is not sufficient to determine that compound nucleus formation is not suppressed - the ER measurements are vital. However, upon increasing Z_pZ_t further, for the systems ^{48}Ca+^{172}Yb (Z_pZ_t = 1400) and ^{50}Ti+^{150}Er (Z_pZ_t = 1496),

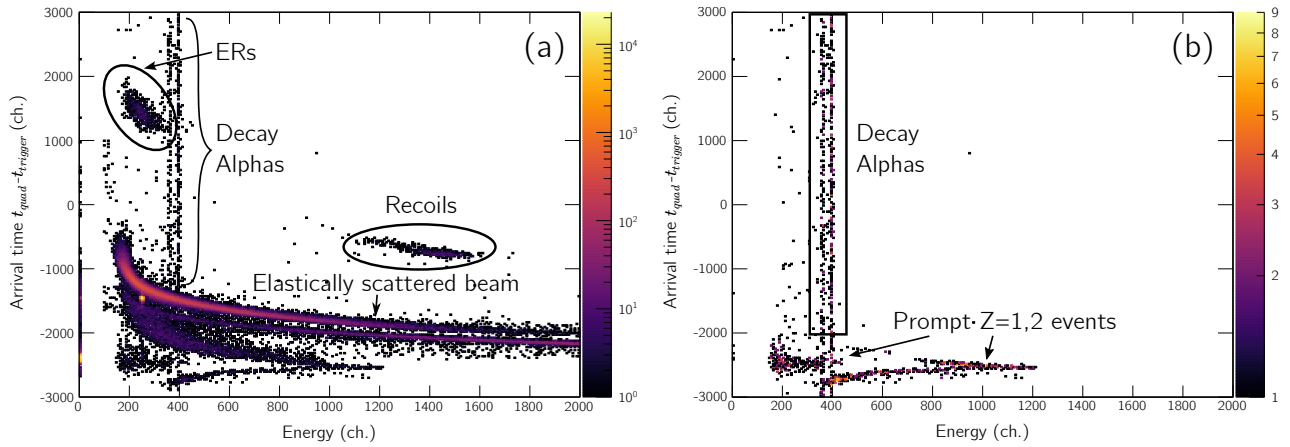

Figure 3. (a) shows energy and arrival time of all events in quadrant 1 of the silicon detector, arising from the reaction ^{30}Si+^{186}W at E_{beam}=140 MeV. ERs, alpha decays, and elastically scattered beam and recoil events are labelled. The pulser (a signal injected into the detector electronics, used for normalisation) is evident as a high-intensity spot near (250,-1500). In (b), the plot is populated with the same data as in (a), but with an anti-coincidence condition on MWPC signals. The gate used to generate the alpha spectra for further analysis is indicated with the black rectangle.

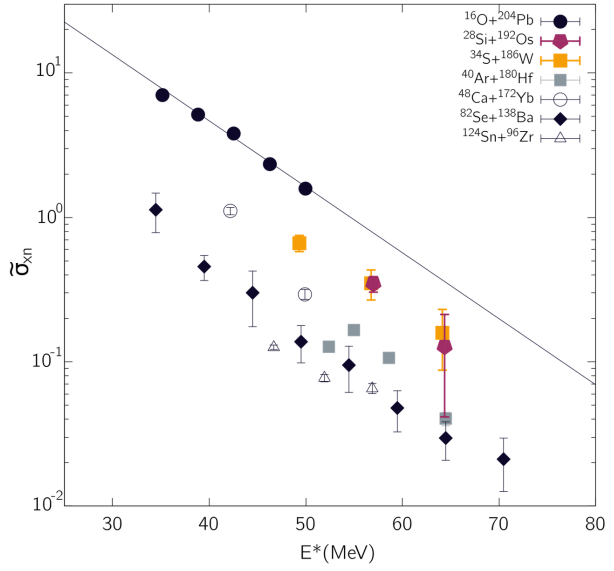

Figure 4. The reduced cross sections originally compiled in Ref. [1] (replicating the symbols and greyscale colours used in that work), along with the new reduced cross sections measured for this work for the reactions ^{28}Si+^{192}Os and ^{34}S+^{186}W (coloured symbols). The major contribution to the uncertainty on the new measurements is statistical.

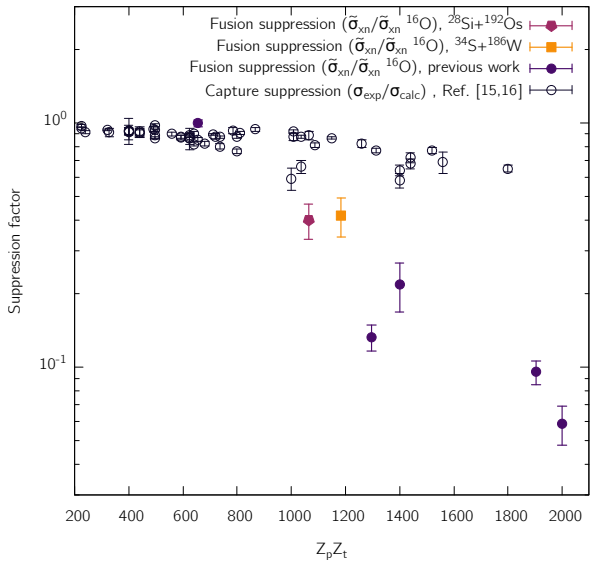

Figure 5. Suppression of fusion (quantified using the $\tilde{\sigma}_{xn}$ measured in this work relative to the $\tilde{\sigma}_{xn}$ of ^{16}O+^{204}Pb measured in Ref. [1]) and of capture (as quantified in Refs. [15] and [16]) as a function of Z_pZ_t. This plot clearly reveals the contrasting behaviour of the fusion suppression, which has a strong exponential dependence on Z_pZ_t, and the capture suppression, which has a much weaker dependence. The two new points added as part of this work clearly define the strong exponential trend between the ^{16}O+^{204}Pb (Z_pZ_t = 656) and ^{40}Ar+^{180}Hf (Z_pZ_t = 1296) systems.

the MADs in Figure 7 show the emergence, and then dominance, of a strong mass-angle correlation.

Without a mass-angle correlation, it may be possible to seek evidence for quasifission in the fission mass widths. The mass widths obtained by taking an angular cut of $120° < \theta_{cm} < 160°$ for all the systems measured for this work (^{16}O, ^{28}Si, ^{34}S and ^{48}Ca-induced reactions) are presented as a function of E^* in Figure 8.

For all three systems, the mass width increases with increasing E^*. This is consistent with the expectation for the behaviour of fusion-fission mass widths presented in previous works [20]. Figure 8 also shows that the mass widths increase with increasing Z_pZ_t. A possible expla-

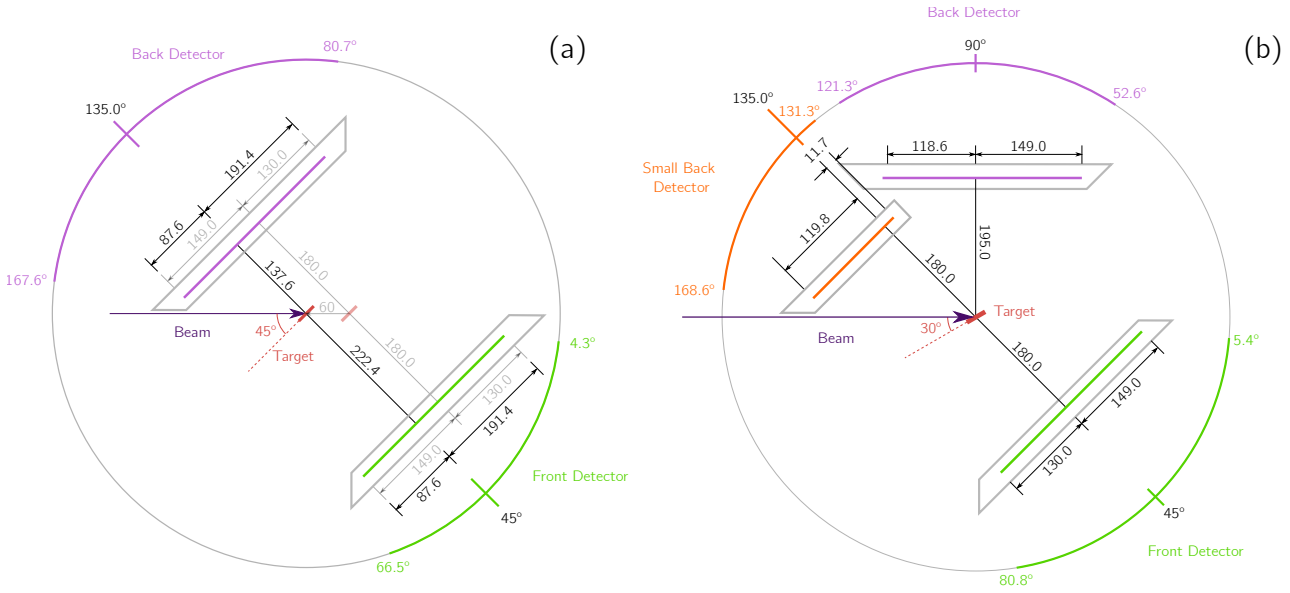

Figure 6. This figure shows a schematic of the CUBE fission spectrometer, in the two configurations used to collect data for this work. The two-detector configuration in (a) was used to collect data for the ^{16}O and ^{34}S-induced reactions, while the more recently added three-detector configuration presented in (b) was used for the ^{28}Si and ^{48}Ca-induced reactions, as well as additional data for the ^{16}O-induced reaction.

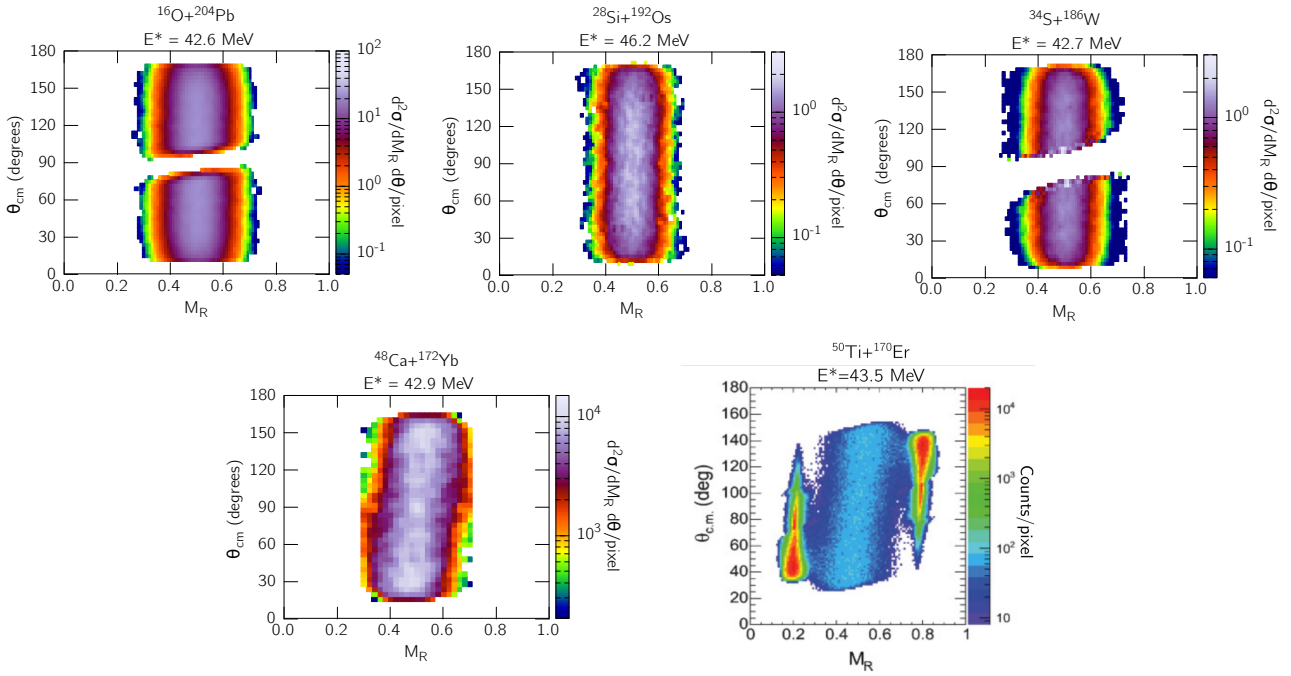

Figure 7. This figure shows a selection of the MADs produced for this work, at similar excitation energies, along with a MAD from Ref. [11] for the ^{50}Ti+^{170}Er reaction, which also produces ^{220}Th as a compound nucleus. The black rectangle over the ^{48}Ca+^{172}Yb MAD identifies the region of the MADs used to obtain the fission mass widths, presented in Figure 8. Detector angular coverage is the reason for the gaps around $\theta_{cm} = 90°$ in the data for the ^{16}O and ^{34}S-induced reactions.

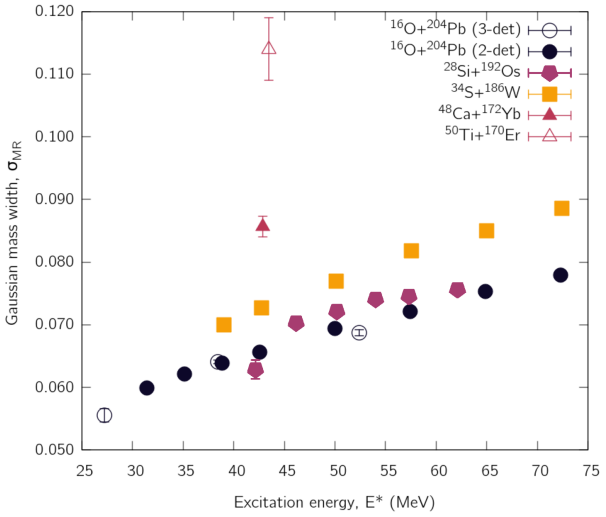

Figure 8. The fission mass widths of the reactions examined for this work: ^{16}O+^{204}Pb, ^{28}Si+^{192}Os, and ^{34}S+^{186}W. The single points are for the reactions ^{48}Ca+^{172}Yb and ^{50}Ti+^{170}Er [11]. For the ^{16}O+^{204}Pb reaction, two sets of measurements were obtained, with CUBE in both a 2-detector and 3-detector configuration.

nation for this trend is the increased angular momentum brought in by progressively heavier projectiles, but previous works have shown (via coupled channels calculations) that the difference in angular momentum is not expected to be large enough to account for the increase in the mass widths for similar systems [9, 11, 21]. Thus, thorough quantitative analysis of the mass widths may provide the only evidence of fusion suppression via slow quasifission in fission characteristics.

4 Conclusions

The ability to measure both the ER cross sections and the fission characteristics of systems forming the compound nucleus ^{220}Th has resulted in two major conclusions from this work. First, that compound nucleus formation can be strongly suppressed without evidence of a mass angle correlation - a conclusion for which the ER measurements were essential. Second, the evolution of the fission characteristics - from a narrow peak with centroid at mass symmetry uncorrelated in mass and angle, to a widening of the distribution in mass, to the emergence and then dominance of a mass-angle correlation - supports the argument that there is a corresponding evolution in the nonequilibrium processes suppressing fusion.

The fission mass widths provide an indication of the onset of this evolution with Z_pZ_t. The change in this quantity is the only signature of compound nucleus suppression evident in the fission characteristics at small Z_pZ_t, even when fusion was measured to be suppressed by a factor of 2.5. This makes the mass widths a potentially sensitive probe to the earliest onset of nonequilibrium outcomes, but requires experimental data for a reaction forming the same CN with low Z_pZ_t.

References

[1] D.J. Hinde, M. Dasgupta, A. Mukherjee, Severe inhibition of fusion by quasifission in reactions forming 220Th, Physical Review Letters **89**, 282701 (2002). 10.1103/physrevlett.89.282701

[2] D. Vermeulen, H.G. Clerc, C.C. Sahm, K.H. Schmidt, J.G. Keller, G. Münzenberg, W. Reisdorf, Cross sections for evaporation residue production near the N=126 shell closure, Zeitschrift für Physik A Atoms and Nuclei **318**, 157 (1984). 10.1007/bf01413464

[3] C.C. Sahm, H.G. Clerc, K.H. Schmidt, W. Reisdorf, P. Armbruster, F.P. Hessberger, J.G. Keller, G. Münzenberg, D. Vermeulen, Fusion probability of symmetric heavy, nuclear systems determined from evaporation-residue cross sections, Nuclear Physics A **441**, 316 (1985). 10.1016/0375-9474(85)90036-3

[4] K. Satou, H. Ikezoe, S. Mitsuoka, K. Nishio, S.C. Jeong, Effect of shell structure in the fusion reactions 82Se+134Ba and 82Se+138Ba, Physical Review C **65**, 054602 (2002). 10.1103/PhysRevC.65.054602

[5] D.J. Hinde, M. Dasgupta, E.C. Simpson, Experimental studies of the competition between fusion and quasifission in the formation of heavy and superheavy nuclei, Progress in Particle and Nuclear Physics **118**, 103856 (2021). 10.1016/j.ppnp.2021.103856

[6] R. du Rietz, D.J. Hinde, M. Dasgupta, R.G. Thomas, L.R. Gasques, M. Evers, N. Lobanov, A. Wakhle, Predominant time scales in fission processes in reactions of S, Ti and Ni with W: Zeptosecond versus attosecond, Physical Review Letters **106**, 052701 (2011). 10.1103/physrevlett.106.052701

[7] E. Williams, K. Sekizawa, D.J. Hinde, C. Simenel, M. Dasgupta, I.P. Carter, K.J. Cook, D.Y. Jeung, S.D. McNeil, C.S. Palshetkar et al., Exploring zeptosecond quantum equilibration dynamics: From deep-inelastic to fusion-fission outcomes in 58Ni+60Ni reactions, Physical Review Letters **120**, 022501 (2018). 10.1103/physrevlett.120.022501

[8] P. Vergani, E. Gadioli, E. Vaciago, E. Fabrici, E. Gadioli Erba, M. Galmarini, G. Ciavola, C. Marchetta, Complete and incomplete fusion and emission of preequilibrium nucleons in the interaction of ^{12}C with ^{197}Au below 10 mev/nucleon, Physical Review C **48**, 1815 (1993). 10.1103/PhysRevC.48.1815

[9] A.C. Berriman, D.J. Hinde, M. Dasgupta, C.R. Morton, R.D. Butt, J.O. Newton, Unexpected inhibition of fusion in nucleus–nucleus collisions, Nature **413**, 144 (2001). 10.1038/35093069

[10] N. Bohr, Neutron Capture and Nuclear Constitution, Nature **137**, 344 (1936). 10.1038/137344a0

[11] R.G. Thomas, D.J. Hinde, D. Duniec, F. Zenke, M. Dasgupta, M.L. Brown, M. Evers, L.R. Gasques, M.D. Rodriguez, A. Diaz-Torres, Entrance channel dependence of quasifission in reactions forming 220Th, Physical Review C **77**, 034610 (2008). 10.1103/physrevc.77.034610

[12] L.T. Bezzina, E.C. Simpson, D.J. Hinde, M. Dasgupta, I.P. Carter, D.C. Rafferty, Determination of angular distributions from the high efficiency solenoidal separator SOLITAIRE, Nuclear Instruments and Methods in Physics Research Section A: Accelerators, Spectrometers, Detectors and Associated Equipment **968**, 163872 (2020). 10.1016/j.nima.2020.163872

[13] M. Leino, Gas-filled separators – an overview, Nuclear Instruments and Methods in Physics Research B **204**, 129 (2003). 10.1016/s0168-583x(02)01901-8

[14] M.D. Rodríguez, M.L. Brown, M. Dasgupta, D.J. Hinde, D.C. Weisser, T. Kibèdi, M.A. Lane, P.J. Cherry, A.G. Muirhead, R.B. Turkentine et al., SOLITAIRE: A new generation solenoidal fusion product separator, Nuclear Instruments and Methods in Physics Research A **614**, 119 (2010). 10.1016/j.nima.2009.12.039

[15] J.O. Newton, R.D. Butt, M. Dasgupta, D.J. Hinde, I.I. Gontchar, C.R. Morton, K. Hagino, Systematic failure of the woods-saxon nuclear potential to describe both fusion and elastic scattering: Possible need for a new dynamical approach to fusion, Physical Review C **70**, 024605 (2004). 10.1103/physrevc.70.024605

[16] D.Y. Jeung, D.J. Hinde, E. Williams, M. Dasgupta, E.C. Simpson, R. du Rietz, D.H. Luong, R. Rafiei, M. Evers, I.P. Carter et al., Energy dissipation and suppression of capture cross sections in heavy ion reactions, Physical Review C **103**, 034603 (2021). 10.1103/PhysRevC.103.034603

[17] D.J. Hinde, M. Dasgupta, J.R. Leigh, J.C. Mein, C.R. Morton, J.O. Newton, H. Timmers, Conclusive evidence for the influence of nuclear orientation on quasifission, Physical Review C **53**, 1290 (1996). 10.1103/physrevc.53.1290

[18] J. Tōke, R. Bock, G.X. Dai, A. Gobbi, S. Gralla, K.D. Hildenbrand, J. Kuzminski, W.F.J. Müller, A. Olmi, H. Stelzer et al., Quasi-fission — the mass-drift mode in heavy-ion reactions, Nuclear Physics A **440**, 327 (1985). 10.1016/0375-9474(85)90344-6

[19] D. Jeung, Ph.D. thesis, The Australian National University (2018)

[20] M.G. Itkis, A.Y. Rusanov, The fission of heated nuclei in reactions involving heavy ions: static and dynamical aspects, Physics of Particles and Nuclei **29**, 160 (1998). 10.1134/1.953064

[21] R. Rafiei, R.G. Thomas, D.J. Hinde, M. Dasgupta, C.R. Morton, L.R. Gasques, M.L. Brown, M.D. Rodriguez, Strong evidence for quasifission in asymmetric reactions forming 202Po, Physical Review C **77**, 024606 (2008). 10.1103/physrevc.77.024606